Citric acid crosslinked natural bi-polymer-based composite hydrogels: effect of polymer ratio and beta-cyclodextrin on hydrogel microstructure.

UYANGA, K. A., OKPOZO, O. P., ONYEKWERE, O. S., and DAOUD, W. A.

2020

Citric acid crosslinked natural bi-polymer-based composite hydrogels: Effect of polymer ratio and beta-cyclodextrin on hydrogel microstructure

Kindness A. Uyanga[a], Oghenefego P. Okpozo[b], Okwuchi S. Onyekwere[c], Walid A. Daoud[a]*

[a] *School of Energy and Environment, City University of Hong Kong, Tat Chee Avenue, Kowloon, Hong Kong*

[b] *School of Engineering, Robert Gordon University, Garthdee, Aberdeen, United Kingdom*

[c] *Faculty of Engineering, Federal University Wukari, Wukari, Taraba State, Nigeria*

*Corresponding author, E-mail: wdaoud@cityu.edu.hk (W. A. Daoud).

Abstract

Composite hydrogels based on natural polymers arouse interest as sustainable matrices for the delivery of bioactive materials. This study investigates the possibility of achieving high thermally and hydrolytically stable, well-defined microstructure bi-polymer composite hydrogels using only natural materials at a low energy process. Firstly, citric acid (CA) crosslinked hybrid hydrogel matrices are developed by varying mole ratio of carboxymethyl cellulose (CMC) to chitosan (CSN) by 1:1, 1:2 and 2:1. Then, hydrolytic, thermal and structural properties of the matrices are studied to determine microstructure. Lastly, the matrices are functionalized with beta-cyclodextrin (β-CD), and the effect of β-CD on hydrogels' microstructure and antibacterial activity is examined. Optimum microstructure is found at CMC:CSN=1:1 for CMC~CA~CSN with a gel fraction of 63%, which increases to 82% when reinforced with β-CD. Interestingly, CMC~CA~2CSN exhibits a combination of good crosslinking, super-absorbency (1229.7% water absorbency and 2200% swelling) yet enhanced hydrolytic stability (84.7% gel fraction). Complexation with β-CD propagates the growth of Gram-positive bacterium, Corynebacterium glutamicum

ATCC 13032. Overall, CMC~CA~CSN~β-CD is considered as a green, crystalline, thermally, and hydrolytically stable composite hydrogel matrix.

Keywords: carboxymethyl cellulose, chitosan, hydrogel, beta-cyclodextrin, environmental sustainability

Introduction

Composite hydrogels have received increasing attention due to the ability to incorporate specific and desirable properties through engineering. While primary research interests have been in developing hydrogels to meet specific properties such as enhanced mechanical performance, however, there is a growing concern for the development of green, yet stable and durable, composite hydrogels [1-4]. In this regard, natural polymers, non-toxic crosslinkers, other safe naturally sourced materials, as well as 'green approaches' have been incorporated to reduce the toxicity level of composite hydrogels [3, 5-9]. Granted, hydrogels made using only natural materials are challenging to fabricate and exhibit poor thermal, crystalline and gel fraction properties [10, 11]; hence the continuous incorporation of synthetic materials. An alternative could be to replace the synthetic polymer hydrogel components [12] with green, low cost, natural components, and vary the ratio of natural polymer components to develop a bi-polymer composite hydrogel with desirable properties. This alternative can be a suitable choice for the development of safe, natural bi-polymer based composite hydrogels.

Natural bi-polymer based composite hydrogels are three-dimensional hydrophilic structures composed of two natural polymers, non-cytotoxic crosslinking agents and a safe solvent of water. They can absorb water and other biological fluids many times their dry weight, yet remain insoluble in the fluids [13]. Water absorbency

depends on factors such as polar functional groups (-OH, -NH_2, -COOH, -$CONH_2$, and -SO_3H), capillary effect, crosslinking density, osmotic pressure, salt content, and impurities in their structure [6, 14, 15]. Insolubility is directly proportional to crosslinking density.

Carboxymethyl cellulose (CMC) [16-19], chitosan (CSN) [20-22], and citric acid (CA) are well-documented materials suitable for development of natural bi- polymer based composite hydrogels. In common, these materials are naturally abundant, low cost, biodegradable, and biocompatible. CMC, a cellulose derived polysaccharide, has a variety of effective functional groups such as -COOH and -OH groups [10, 14, 23, 24]. It is also a polyelectrolyte cellulose suitable for controlled release of loaded materials. CSN, a derivative of chitin, is a cationic polymer with anti-microbial properties [25, 26]. In biomedicine, CSN is used as backbone for the synthesis of antibacterial hydrogels for drug delivery and wound dressing/treatment [4, 26, 27]. The mutual attraction between the positive charge of CSN and the

negative charge microbial cell membrane surfaces lead to bacterial growth inhibition. In biotechnology, CSN serves as a feedstock for *C. glutamicum* in the production of amino acid, alcohols, organic acids, polymers, such as diamines and polyhydroxy butyrate, and proteins such as, α-Amylase [28-31]. *C. glutamicum* utilizes carbohydrate derivatives, such as N-acetyl-glucosamine, as its carbon source [28]. Hybridization of CSN with CMC introduces COOH groups at the glucosamine unit, which enhances gel fraction of the bi-polymer hybrid [19, 32]. It also increases antimicrobial and antioxidant properties [33]. CA is a carboxylic acid used as a crosslinking agent to enhance hydrogel hydrophilicity and stabili ty to prevent components leaching from hydrogel microstructure [34]. Super-absorbency of CA crosslinked hydrogels is due to electrostatic repulsion between the COOH groups of

CMC and the CA [35, 36]. When used as a crosslinker for CMC and CSN hybrid, the crosslinking mechanism is esterification resulting in the formation of -COOR bonds, with/without a few peptide bonds which are medically important molecules [36]. β-CD is a low cost, natural polymer with good biocompatibility, no toxicity, low water solubility and high entrapment efficiency. It is a cyclic oligosaccharide made up of seven dextrose units containing a hydrophobic central cavity and a hydrophilic outer surface [37, 38]. This structural characteristic makes β-CD excellent for improving loading, swelling, reinforcement and prolonging the release of materials [35, 39, 40]. Also, β-CD has been reported to have low or almost zero antimicrobial activity [41-43] especially against Gram-positive bacteria such as *S. ambofaciens* ATCC 23877 [43], and *S. aureus* [44]. To enhance fixation of hydrophobic agents as well as crosslinking, β-CD was selected to be incorporated into the hydrogel matrices. Natural bi-polymer composite hydrogels synthesized by the unique synergy of CMC, CSN, CA and β-CD can open up pathways for the development of safe, durable, and sustainable composite hydrogel matrices.

In this study, CMC-CSN, β-CD and CA were used as bi-polymer hydrogel backbone, functional component, and crosslinking agent, respectively to synthesize composite hydrogel matrices. The detailed objectives of this study were to (1) synthesize environmentally sustainable citric acid crosslinked carboxymethyl cellulose-chitosan (CMC-CSN-CA) composite hydrogel matrices by varying mole ratio of the natural polymers; (2) characterize the synthesized hydrogels to determine optimum microstructure and evaluate the effect of varying the polymer ratio on the hydrogels' properties; and (3) reinforce the hydrogel matrices with β-CD and study the effect of β-CD on hydrogels' properties and microstructure. In this study, a

promising natural composite hydrogel with high hydrolytic and thermal stability, is developed.

2. Experimental

2.1 Materials

Carboxymethyl cellulose sodium (degree of substitution, DS = 0.77, average molecular weight, Mw= 250 kDa and viscosity at 25 ℃ = 700 ± 50 mPas) was purchased from Alfa Aesar (Heysham, England). Chitosan (viscosity = 5-20 mPas, 0.5% in 0.5% acetic acid at 20 ℃) and beta-cyclodextrin (DS = 0.62, viscosity at 25 ℃ = 20 ± 5 mPas) were obtained from Tokyo Chemical Industry Co. Ltd. (Tokyo, Japan). Anhydrous citric acid was purchased from Energy Chemical Company (Shanghai, China). All chemicals were of analytical purity and were used as purchased without further purification. De-ionized water (18.2 MΩ cm) was used as a solvent for fabricating the hydrogels.

2.2 Preparation of CMC-CSN-CA hydrogel matrices

The composite hydrogel matrices were prepared by chemical gelation method at 25 ℃. Three CMC-CSN bi-polymer solutions were prepared with CMC:CSN as 1:1, 1:2, and 2:1, respectively. First, 0.5 g of CMC was dissolved in 100 mL de-ionized water for 1 h under magnetic stirring until CMC was fully dissolved, and 0.3 g of CA was dispersed in 100 mL deionized water under magnetic stirring for 30 mins. Second, 0.5 g of chitosan was dissolved in 1 wt.% acetic acid solution for 1 h at 25 ℃ under magnetic stirring. Third, 10 mL, 10 mL and 20 mL of the homogenous CMC solutions were separately measured into three vial bottles; and 5 mL CA solution was added into the different CMC solutions to form CMC-CA crosslinked solutions, and labelled CMC~CA, CMC~CA, and 2CMC~CA, respectively. Then, 10 mL, 20 mL,

and 10 mL of the CSN solution were measured into three different beakers and stirring was continued using magnetic stirrers. While under stirring, CMC~CA, CMC~CA and 2CMC~CA were added dropwise into the 10 mL, 20 mL, and 10 mL CSN solutions, respectively to form composite hydrogel matrix solutions labelled CMC~CA~CSN, CMC~CA~2CSN, and 2CMC~CA~CSN. CMC~CA~CSN,
CMC~CA~2CSN, and 2CMC~CA~CSN were poured into moulds, allowed to stand overnight, and dried using a vacuum oven at 60 ℃. The hydrogel composites synthesized were washed, put back to dry in the vacuum oven for 24 h, and then, stored in the desiccator.

2.3 Preparation of CMC-CSN-CA-β-CD hydrogels

CMC~CA~CSN, CMC~CA~2CSN, and 2CMC~CA~CSN composite hydrogel matrices were synthesized (following Section 2.2). Also, 0.3 g of β-CD was dissolved in 100 mL de-ionized water. Then, 3 mL of the β-CD solution was added into each of CMC~CA~CSN, CMC~CA~2CSN, and 2CMC~CA~CSN composite hydrogel matrix solutions. The solutions were stirred for 6 h, poured into moulds, and allowed to stand overnight at room temperature to remove entrapped gas. The hydrogels were also dried, washed, and stored following the same procedure described in Section 2.2.

2.4 Characterization of CMC-CSN-CA hydrogel matrices

The dried hydrogel matrices were characterized for swelling (%), water absorbency (%) and gel fraction (%). The matrices were incubated in de-ionized water at 25 ℃ for 48 h. The swelling weights of the hydrogel matrices were measured gravimetrically after wiping excess water from the hydrogel surface. Weights were taken every hour within the first 7 h and at 48 h. At 48 h, excess water was drained

for 10 mins. Water absorbency (A_w) of the matrices (percentage) was calculated using Equation 1.

$$A_w = (W_s – W_d)/W_d \quad (1)$$

where W_s and W_d are the weights of the swollen composite hydrogel and the corresponding dry composite hydrogel, respectively. The water uptake measurements were done three times for each composite hydrogel matrix, and the average of the three values was recorded. Further, a mass of dried hydrogel matrix was immersed in de-ionized water for 48 h at 25 ℃. The insoluble part necessary for assessing the hydrolytic stability of the hydrogel samples was dried and weighed. Gel fraction (G_f) of the matrices (percentage) were calculated according to Equation 2.

$$G_f = (W_i/W_d) \quad (2)$$

where W_i is the weight of the dried insoluble part, and W_d is the weight of dried matrix before immersion in water.

Furthermore, the prepared hydrogel matrices were characterized by X-ray diffraction (XRD), Fourier transform infra-red spectroscopy (FTIR), scanning electron microscopy (SEM), differential scanning calorimetry (DSC) and thermographic analysis (TGA). The XRD patterns of the composite hydrogel matrices in the scanning range of $10° \leq 2\theta \leq 60°$ were obtained using a PANalytical X'Pert^3 Powder (PANalytical, Netherlands) equipped with a CuKα radiation source, operated at 40 kV and 40 mA. The functional groups of the composite hydrogels were characterized using FTIR spectrometer (IRAffinity-1, Shimadzu, Japan). All samples were analyzed as powder, thoroughly mixed with KBr powder, compressed into 1 mm transparent pellet, and analysed over the range of 4000 to 400 cm^{-1}. Surface morphologies of the

synthesized hydrogel matrices were investigated using FEI Quanta 450 FESEM (FEI Co., Europe), operated at an accelerating voltage of 10 kV. The samples were gold-sputtered before analysis. Thermal analysis of the hydrogel matrices was conducted using the Mettler Toledo Thermographic and Differential Scanning Calorimetry (TGA/DSC) 1 (Mettler Toledo, Switzerland). The samples were heated at a heating rate of 5 ℃ min^{-1} over a temperature range of 25 to 500 ℃ under a nitrogen flowrate of 50 ml min^{-1}.

2.5 Characterization of synthesized composite CMC~CA~CSN~β-CD hydrogels

To confirm crosslinking density and internal network formation, the synthesized CMC-CA-CSN-β-CD hydrogels were characterized for hydrolytic properties. Thermal stability and chemical structure were also analyzed using DSC- TGA, and FTIR (following Section 2.3). The chemical interaction and molecular structure were further confirmed using Raman spectroscopy. An Avalon Instruments Raman Station (Avalon RAMANITATION R3, Belfast) was used to obtain the Raman spectra of the hydrogels using an excitation wavelength of 785 nm. Laser power of the source was maintained at 300 mW for 20 s. The spectral range was 300 – 3200 cm^{-1}. Antimicrobial activity of the developed hydrogels was also examined using solid gel dynamic shake flask method. Corynebacterium glutamicum ATCC 13032, a Gram-positive bacterium, was grown in 5 mL of Luria-broth (LB) media (inoculation at 1% V/V) in a shaking incubator overnight at 30 ℃ and 200 rpm. After that, 0.1 ml of the grown culture was added into 1000 mL of sterile de-ionized water (18.2 MΩ- cm), and this was aliquoted at 50 mL into 160 mL serum bottles containing the test

materials. The bottles were then capped with aluminium foil and were put into shaking incubator for 2 hours at 30 ℃ and 200 rpm. Subsequently, colony-forming

unit (CFU) per mL of the test cultures were determined by serial dilution and spreading onto LB agar plate.

3. Results and discussion

3.1 Hydrogel synthesis

Fig. 1 illustrates the hydrogel synthesis procedure.

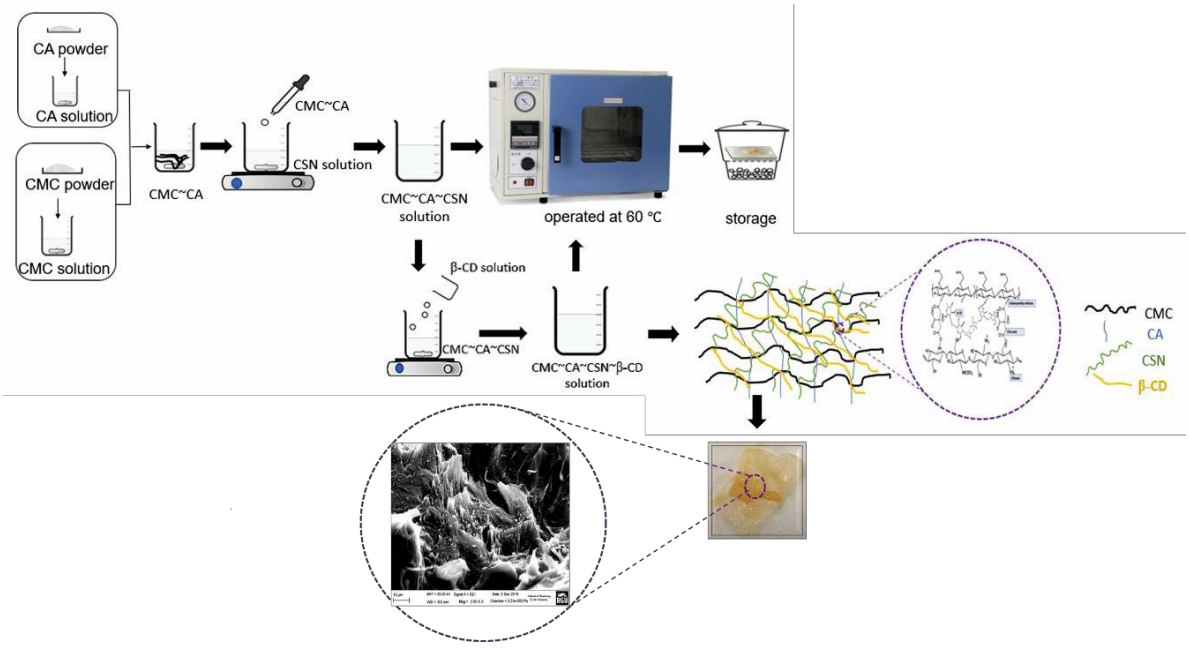

Figure 1 Synthesis procedure of CMC~CA~CSN~β-CD hydrogels

3.2 Effect of varying mole ratio of polymers on properties of CMC-CA-CSN matrices

3.2.1 Hydrolytic properties

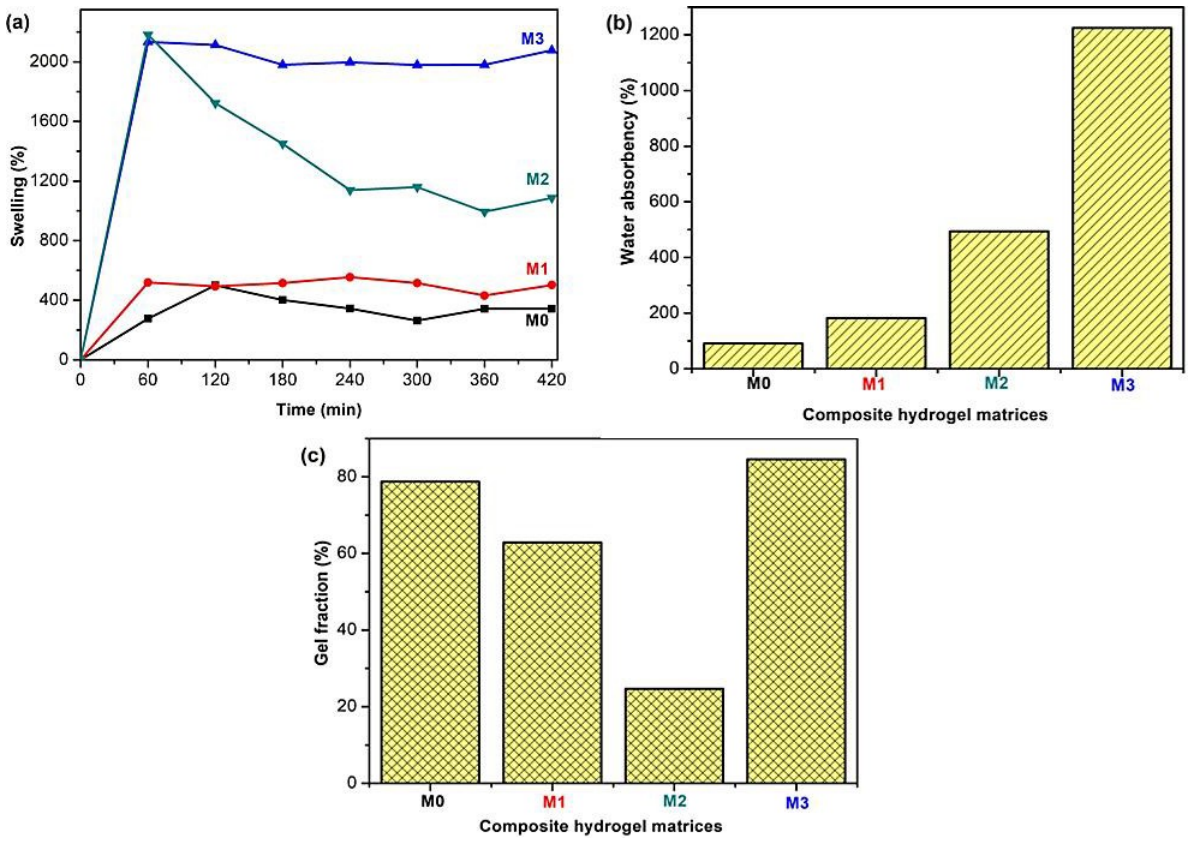

Fig. 2. Hydrolytic properties of the hydrogel matrices (non-crosslinked (M0), CMC~CA~CSN (M1), 2CMC~CA~CSN (M2), and CMC~CA~2CSN (M3)) in de-ionized water at 25 ℃ (a) swelling (%), (b) water absorbency (%), and (c) gel fraction (%).

Swelling, water absorbency, and gel fraction (at 25 ℃) of the prepared hydrogel matrices are shown in **Fig. 2**(a-c). The hydrolytic properties were carried out to assess the degree of crosslinking network and select optimal hydrogel matrix. Crosslinking density is inversely proportional to swelling and water absorbency. Increasing mole ratio of either CMC and CSN to 2, increased swelling (**Fig. 2**a)and water absorbency (**Fig. 2**b). At CMC:CSN = 1:2, CMC~CA~2CSN exhibited maximum swelling combining good crosslinking degree, super-absorbency (2200% swelling, 1229.7% water absorbency), and enhanced hydrolytic stability (84.7% gel fraction), and surpassing reported performances of some natural-synthetic or

synthetic-synthetic polymer-based composite hydrogels (see **Table S1** in Supplementary information) [45-48]. Conversely, at CMC:CSN = 1:1, matrix CMC~CA~CSN (495% swelling, 177% water absorbency) showed the least swelling. The dried CMC-CSN-CA hydrogel matrices swelled quickly within the initial 60 min and attained equilibrium swelling in 2 h (M1), 4 h (M2), and 3 h (M3). Swelling is due to the presence of an increased number of hydroxyl and ester functional groups introduced by crosslinking the CMC~CSN backbone with CA [36, 47, 49]. Hydrolytic stability of the hydrogel matrices is shown in **Fig. 2**c. M0 had 79% insoluble parts in water after 48 h. Crosslinking with CA, the matrices had insoluble parts 63% (M1), 24% (M2), and 85% (M3). The result shows that increasing the mole ratio of CMC in the composition increased the dissolution of the hydrogel matrices while increasing the mole ratio of CSN decreased dissolution. The gel fraction result, thus, suggests that hybridization of CMC with CSN (1) improved stability of CMC-CSN composite in de-ionized water, and (2) minimized instability of CMC in the presence of CA. Dharmalingam *et al.* [5] reported that crosslinking of CMC alone with CA resulted in

intramolecular crosslinking due to repulsive force exerted by $-COO^-$ groups which lead to increased solubility of the hydrogels. Hence, the increased water stability of M3 could be attributed to increased mole ratio of CSN, which is water-insoluble in the CMC-CSN hybrid [32].

Hence, the swelling, water absorbency and gel fraction results show that (1) M1 has the optimal microstructure; (2) M3 is superabsorbent yet hydrolytically stable, and (3) hybridization with CSN enhances the stability of CMC-CSN composite hydrogel matrices in de-ionized water. Importantly, the enhanced gel fraction of M3 highlights the potential and positive outlook for the replacement of synthetic polymers with natural polymers for the fabrication of safe, durable hybrid hydrogels.

3.2.2 Chemical properties

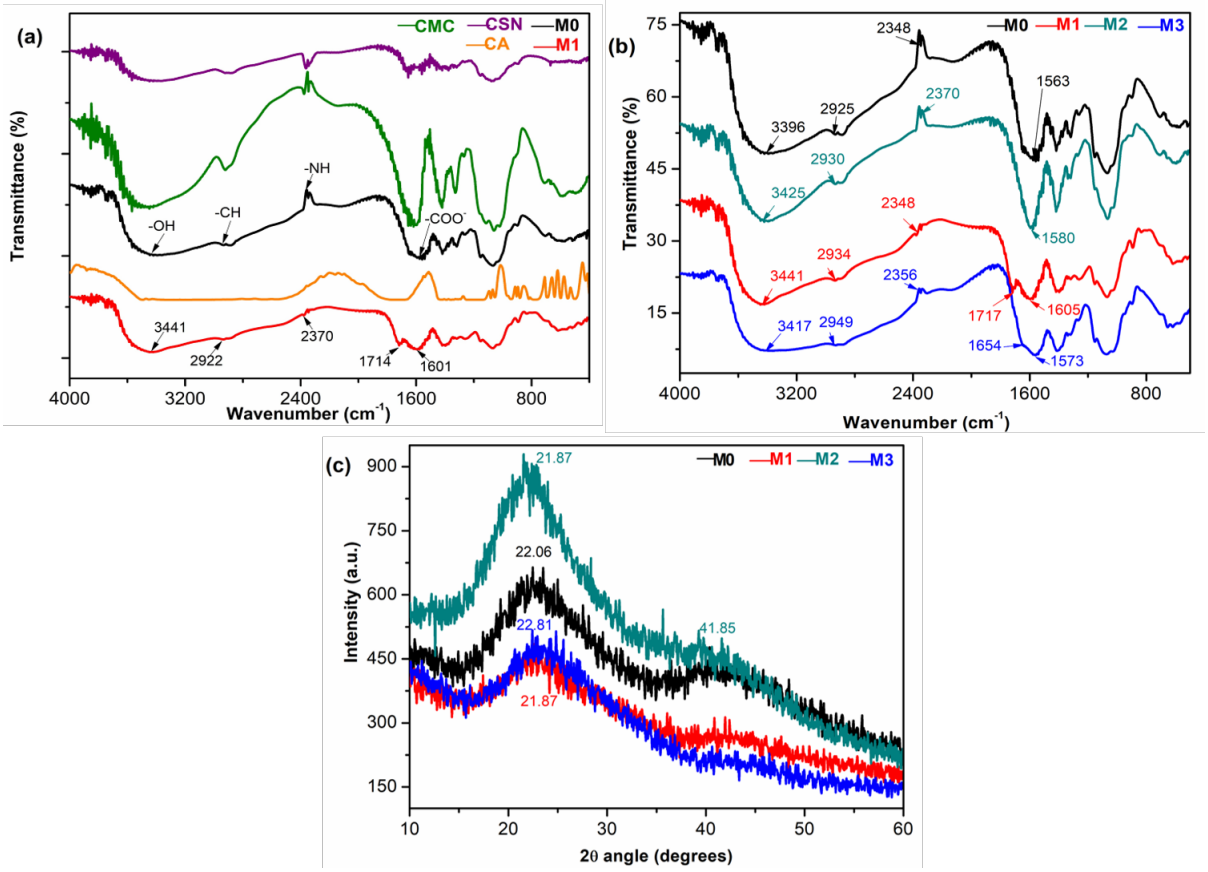

Fig. 3. (a) FTIR of CMC, CSN, hybrid polymer CMC-CSN (M0), CA, and the hydrogel matrix, CMC~CA~CSN (M1). (b) FTIR of CMC-CSN (M0) and the citric acid crosslinked hydrogel matrices. (c) XRD patterns of CMC-CSN (M0) and the composite hydrogel matrices at different ratios of CMC to CSN equals 1:1 (M1), 2:1 (M2), and 1:2 (M3).

To confirm the internal structure, miscibility, crosslinking and functional groups, FTIR spectra and XRD patterns of the non-crosslinked bi-polymer backbone and the hydrogel matrices were recorded. In the FTIR spectra (**Fig. 3**a and b), the broad band at 3600-3200 cm^{-1} corresponds to the stacking of -OH and -NH stretching vibrations of CMC and CSN [50-53]. For M1 (**Fig. 3**a), the peaks at 2934 cm^{-1} and 2890 cm^{-1}, 2348 cm^{-1}, 1717 cm^{-1}, and 1605 cm^{-1} are attributable to asymmetrical and symmetrical -CH stretching vibrations, carbonyl bond of ester formed, and $-COO^{-}$

group. M1 exhibited mixed characteristics of CMC, CSN, and CA, confirming crosslinking and chemical interaction [23, 51]. For example, the weakened characteristic absorption band of CMC at 1000-1200 cm^{-1} indicate the participation of the -OH group of CMC in the chemical reaction. However, the intensity of the ester bond decreased in M3 at CMC:CSN = 1:2 and disappeared in M2 at CMC:CSN = 2:1 (**Fig. 3**b). Thus, the presence of ester bonds in only the spectra of M1 and M3 confirms (1) miscibility and enhanced crosslinking density, and (2) the swelling and water absorbency results in Section 3.1.1 [14, 35, 36]. M1 and M3 also show broad peaks at 3441 cm^{-1} and 3417 cm^{-1}, respectively, attributable to -OH stretching. Also, compared with the spectra of the non-crosslinked hydrogel backbone, M0, the typical peaks of the hydrogel matrices are shifted towards higher wavenumbers indicating the presence of different hydrogen bond strengths. M1 has peaks shifted towards higher wavenumbers. This indicates that of the three matrices synthesized, M1 had the strongest bond formation since more energy was required to cause vibrations of the bonds recorded in the spectra. The FTIR spectra for CMC, CSN, and CA are like those reported by other authors [50, 51, 54, 55]. **Fig. 3**(a and b) thus, confirms that

M1 exhibited enhanced miscibility and internal network compared to other hydrogel matrices developed. The XRD patterns (**Fig. 3**c) show that the hydrogel matrices exhibit different degrees of crystal growth. Remarkably, all of the developed hydrogel matrices are semi-crystalline -a desirable and unique property when compared to those reported for most natural-synthetic composite hydrogels [47]. Without crosslinking, CMC-CSN backbone exhibited two diffraction peaks indicating that it is a hybrid of CMC and CSN. Between 2θ=10 and 60°, CMC shows typical peaks at 2θ=20° while CSN has typical peaks at 2θ=11° and 20° attributable to the amorphous nature of the polymers and the crystalline structure of chitin [51, 54, 55]. **Fig. 3**c

shows that increasing mole ratio of CSN in the composition decreased peak intensity but increased peak width of the hydrogel matrices. And, increasing the mole ratio of CMC increased peak intensity and narrowed peak width. Thus, crystallinity peak for M0 at 2θ=22.81° was gradually broadened with increasing mole ratio of CSN to give peaks for M1 and M3 at 2θ=21.87 °. Peak broadening occurs with increasing crosslinking or internal strain [5], and peak intensity and width in the XRD pattern of a sample have a close correlation with the materials' crystallinity [55]. The peaks of the hybrid hydrogel matrices show transformation toward crystalline nature due to crosslinking the composite polymers with CA. Thus, M1 and M3 exhibited some degree of favourable crystal growth due to intramolecular and intermolecular hydrogen bonds from functional groups introduced by hybridization of CMC and CSN polymer chains and crosslinking with CA.

3.2.3 Thermal stability

DSC and TGA were used to determine the thermal stability of the composite hydrogel matrices and illustrated in **Fig. 4**. Effect of varying mole ratio of CMC and CSN on the thermal stability of the hydrogels was also observed. The DSC results (**Fig. 4**a) show that crosslinking with CA enhanced thermal stability of the hydrogel matrices. And, increasing the mole ratio of CMC in the hydrogel composition increased endothermic property of the hydrogel matrix as seen with M2 between 25- 170 ℃. However, above 275 ℃, M2 became more exothermic when compared with M3. Maximum heat flow was 16.38 mW and 8.15 mW for M2 and M3, respectively. Crosslinking the hybridized monomers enhanced stability towards heat for the hydrogel matrices [54]. Thermal degradation of the matrices was studied with TGA (**Fig. 4**b). As shown in **Fig. 4**b, the hydrogel matrices are thermally stable up to 500 ℃. Three stages of degradation were observed for the hydrogel matrices and the

backbone, M0. The first (25-250 ℃) and second (250-317 ℃) mass losses are due to the removal of free and bound water in the hydrogel matrices. The third (317-500 ℃) mass loss is due to actual decomposition of components of the hydrogel matrices. Maximum weight loss of the samples was observed at 317 ℃ in the second step. The weight of the hydrogel matrices only dropped a maximum of 12.6% between 25-250 ℃. The substantial weight loss in the range of 250 -500 ℃ is attributable to the decarboxylation of CMC, partial degradation of CSN and decomposition of CA [5, 15]. The TGA result is similar to those reported in the literature, although in some studies, the first and second degradation stages were considered as a single stage [48]. Given that the weight of the green hydrogel matrices only decreased by 12.6% at 250 ℃, and 5.6% (M0), 4% (M1), 5.6% (M2), and 4.8% (M3) at 50 ℃, the hydrogel matrices are thermally stable.

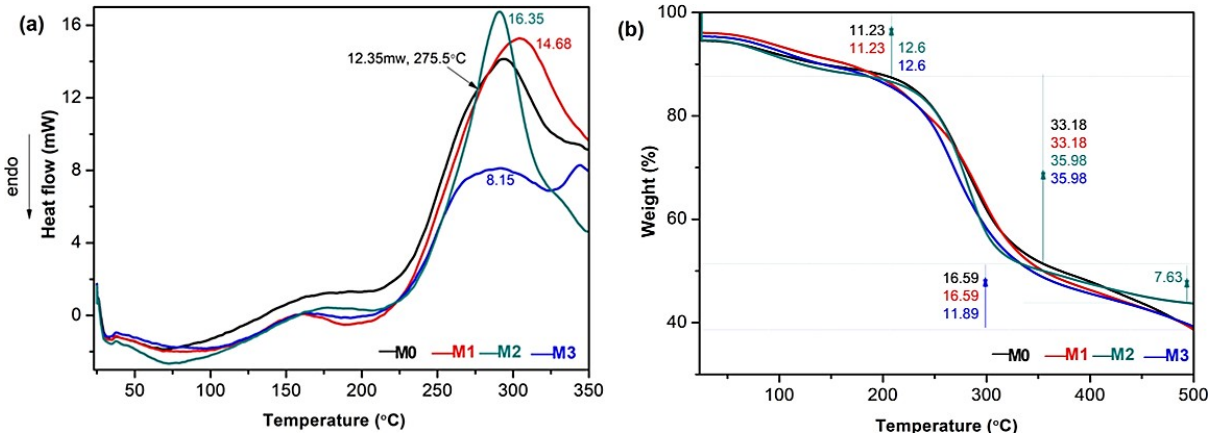

Fig. 4. Thermal analysis (a) DSC and (b) TGA of the hydrogel matrices (non-crosslinked (M0), CMC~CA~CSN (M1), 2CMC~CA~CSN (M2), and CMC~CA~2CSN (M3))

3.2.4 Surface morphology

To further confirm the network formation, the surface morphology (top and cross-sectional views) (**Fig. 5**.) of the crosslinked hydrogel matrices was studied.

The smoother and stable the surface morphology, the better the hydrogels' homogeneity and microstructure. At CMC:CSN = 1:1 (**Fig. 5**ai) and 1:2 (**Fig. 5**ci), the hydrogel matrices exhibited different degrees of surface smoothness. The surface morphology of the CMC~CA~CSN was the firmest and most stable (**Fig. 5**ai) without pin-holes unlike 2CMC~CA~CSN (**Fig. 5**bi). The cross-sectional view of CMC~CA~CSN (**Fig. 5**aii) also showed that it had the best firmly held microstructure. Increasing mole ratio of CMC to 2 increased smoothness of 2CMC~CA~CSN but reduced its stability under the electron beam, hence the observed pinholes. The smoothness, stability, and uniformity of CMC~CA~CSN, therefore, confirms its higher degree of homogeneity, durability, and well-developed microstructure when compared with 2CMC~CA~CSN and CMC~CA~2CSN.

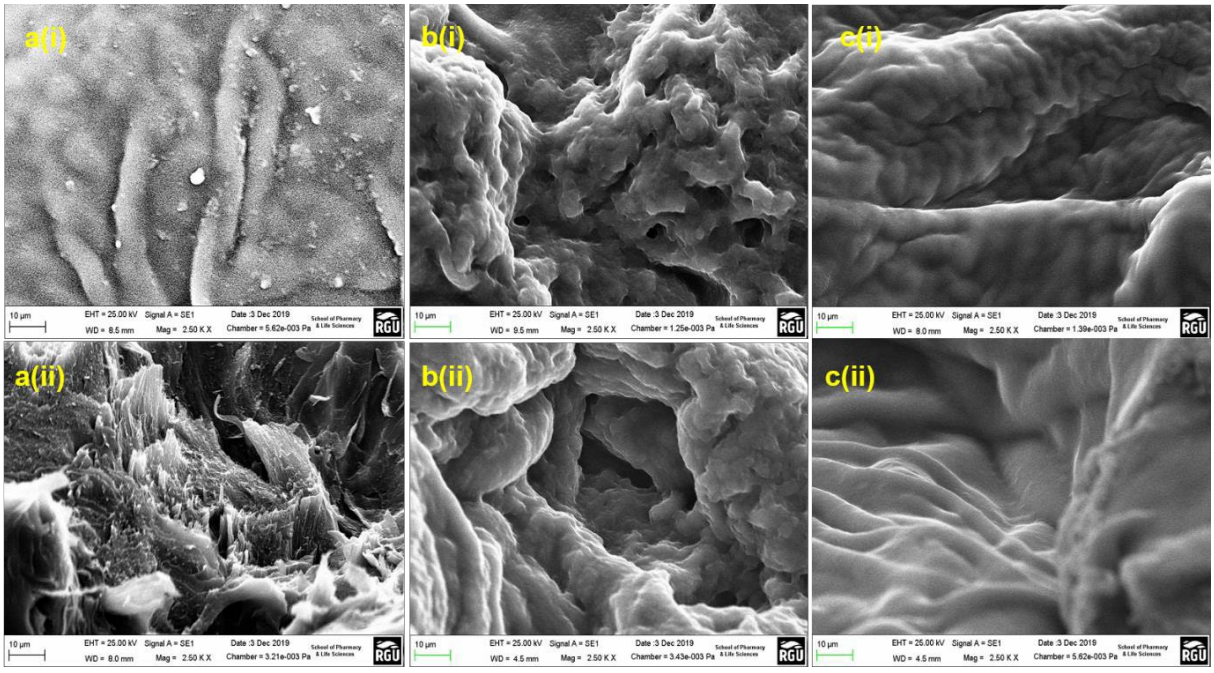

Fig. 5. Micrographs of the crosslinked hydrogel matrices (a) CMC~CA~CSN, (b) 2CMC~CA~CSN, and (c) CMC~CA~2CSN from (i) top view, and (ii) cross -sectional view

From the preceding characterization results, increasing mole ratio of CMC from 1 to 2 increased water uptake indicative of decreased crosslinking density; increased dissolution in de-ionized water at 25 ℃; and decreased thermal and

surface stability. Also, increasing mole ratio of CSN from 1 to 2, although increased water uptake, enhanced insolubility of the hydrogel matrices, thermal stability and crystallinity of the hydrogel matrices, evident with M3. However, maintaining the mole ratio of CMC to CSN at 1:1 yielded the best microstructure with moderate swelling, water absorbency and good resistance to dissolution in water, crystallinity, thermal and surface stability. Overall, keeping the mole ratio of CMC:CSN at 1:1 produced a safe, green, thermally and hydrolytically stable, durable, and well- developed hydrogel matrix, M1. β-CD was incorporated to enhance the potential for the developed matrices to be ideal for wound treatment. The β-CD reinforced matrices were then characterized for hydrolytic properties to study the effect of β-CD on microstructure formation. Thermal stability and chemical structure were also assessed using TGA and FTIR, respectively.

3.3 Effect of β-CD on the developed hydrogel matrices

β-CD is known as an excellent encapsulating material for controlled and prolonged release [35, 37, 39, 40]. The release of loaded agents occurs when the substrate is exposed to a slight increase in temperature triggered by actions such as exposure to sunlight. To confirm the steady release of loaded materials, the β-CD functionalized hydrogels were characterized for hydrolytic properties (i.e. swelling, water absorbency, and gel fraction). Hydrolytic performance is also essential to ascertain the crosslinking density microstructure formation, thermal stability and chemical structure. **Fig. 6** illustrates the effect of incorporating β-CD on hydrogel properties.

Hydrolytic properties characterization (**Fig. 6**a-c) show that β-CD in the hydrogel matrices (M1, M2, and M3) increased hydrolytic stability for hydrogels H1,

H2, and H3; and swelling (%) and water absorbency (%) for H2. Equilibrium swelling for H1 and H3 were attained at 300 min. **Fig. 6**a shows that hydrogel matrix without β-CD (H0), and hydrogel H2 with β-CD (and CMC:CSN =2:1) were unstable, exhibiting high swelling, water absorbency, and high dissolution after 48 h. Thus, the hydrolytic analyses indicate that incorporation of β-CD (1) enhanced the degree of crosslinking for hydrogels H1 and H3, and (2) H1 maintained the best microstructure formation with optimum water absorbency (116%) and gel fraction (82 %). This result agrees with that of Kono *et al.* [50] that β-CD improves stability towards heat and insolubility. Like in Section 3.2.1, the gel fraction was enhanced for H3 (at CMC:CSN = 1:2). The increased amount of CSN in the composition could have minimized the bi-polymer interaction with water molecule leading to an increased gel fraction (95.15%) after 48 h in de-ionized water. Hybridization of CMC with CSN at CMC:CSN=1:2 could have introduced mechanical properties such as elasticity, stiffness, rigidity, and resistance as shown in Supplementary data **Figure S**1. This result further highlights the potential positive outlook for the replacement of synthetic polymers with natural polymers for the fabrication of composite hydrogels.

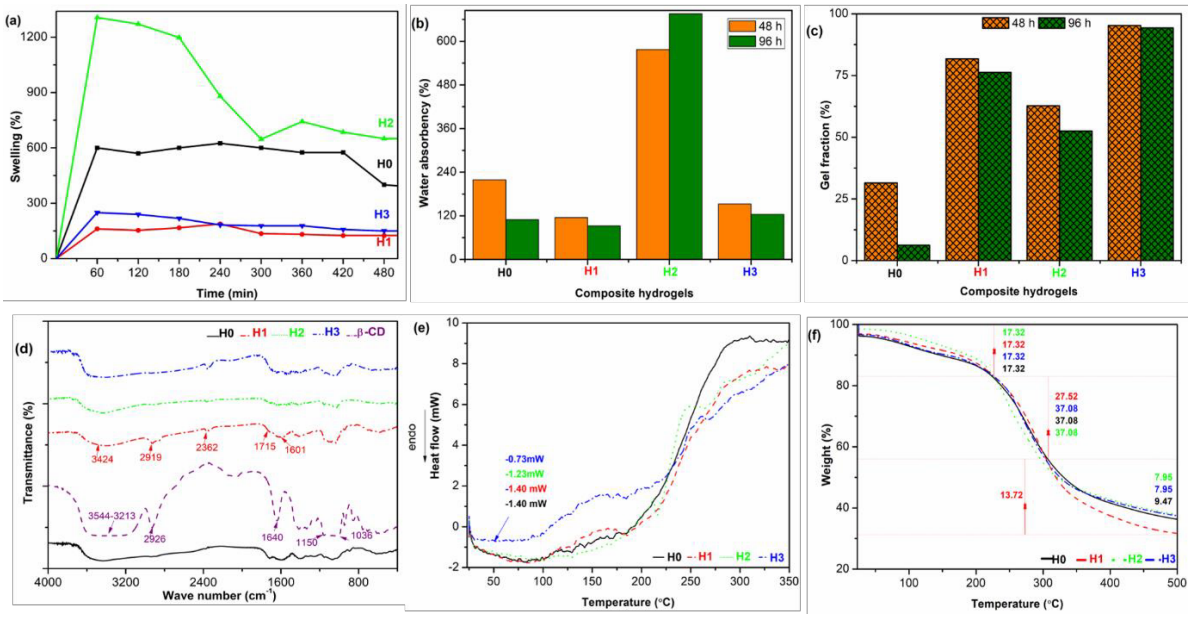

Fig. 6. Effect of incorporating β-CD on (a) swelling (%) (b) water absorbency (%) (c) gel fraction (%) (d) transmittance (e) heat flow and (f) mass loss for the synthesized composite hydrogels H0 (CMC~CA~CSN), H1 (CMC~CA~CSN~β-CD), H2 (2CMC~CA~CSN~β-CD), and H3 (CMC~CA~2CSN~β-CD).

The FTIR spectra (**Fig. 6**d) further confirms that H1 exhibited enhanced miscibility, crosslinking, and chemical structure indicative of well-developed microstructure. H1 exhibit a combination of characteristic peaks of H0 and β-CD and had peaks of varied intensities and shifts in wavenumbers. The FTIR spectra of pure β-CD showed a broad peak between 3544 cm^{-1} and 3213 cm^{-1} ascribable to -OH group stretching, and an intense peak at 2926 cm^{-1} attributable to -CH stretching vibrations. Other peaks observed at 1640 cm^{-1}, 1150 cm^{-1}, and 1036 cm^{-1} can be ascribed to -HOH deformation bands of water present in β-CD, -CH overtone stretching, and -COC vibrations respectively. This result agrees with those reported by others [40, 50]. H1 had peaks at 3424 cm^{-1}, 2919 cm^{-1}, 2362 cm^{-1}, 1715 cm^{-1}, and 1601 cm^{-1} attributable to -OH stretching vibrations, -CH stretching vibrations, -NH group, carbonyl bond of ester formed, and $-COO^{-}$ group. The new sharp peaks at 2919 cm^{-1} and 1601 cm^{-1} due to -CH stretching vibration and -HOH deformation bands of water of β-CD present only in H1 gives further proof of improved crosslinking. Based on the FTIR spectra, we conclude that H1 alone clearly demonstrates sharp peaks related to β-CD shifted to either lower or higher wavenumbers indicative of successful formation and structural change of CMC~CA~CSN~β-CD composite hydrogel.

Fig. 6(e and f) illustrate the thermal properties of the composite hydrogels after β-CD was added. **Fig. 6**e shows that addition of β-CD did not affect the thermal stability of H1 at 25-120 ℃. A slight increase in exothermic property was observed

afterwards at 120-175 ℃. However, to a large degree (at least 56% at 50 ℃), β-CD incorporation increased exothermic behaviour of H3 at 25-225 ℃. It could be that as temperature increased for H3, dehydration of the loosely held -HOH deformation bands of water in β-CD occurs, leading to the evolution of heat. At 50 ℃, heat flows for H0, H1, H2 and H3 are -1.40 mW, -1.40 mW, -1.23 mW and -0.73 mW, respectively. The TGA curves (**Fig. 6**f) show three stages of thermal degradation between 25-227 ℃, 227-357 ℃, and 357-500 ℃ due to loss of free water, bound water, and degradation of the polymeric materials, respectively. At 50 ℃, mass losses for hydrogels H0 (4.2%), H1 (2 .3%), H2 (1.7%), and H3 (3.9%) indicate that the hydrogels are thermally stable enough for wound treatment. Mass loss at the end of the first degradation stage for the three hydrogels developed was 17.32% at 227 ℃. There is no evidence of similar studies in the literature; hence, our pioneer study results for thermal stability cannot be compared yet. However, results on the three stages of thermal degradation agree with those published for pure CMC and CSN polymer-based hydrogels [5, 15].

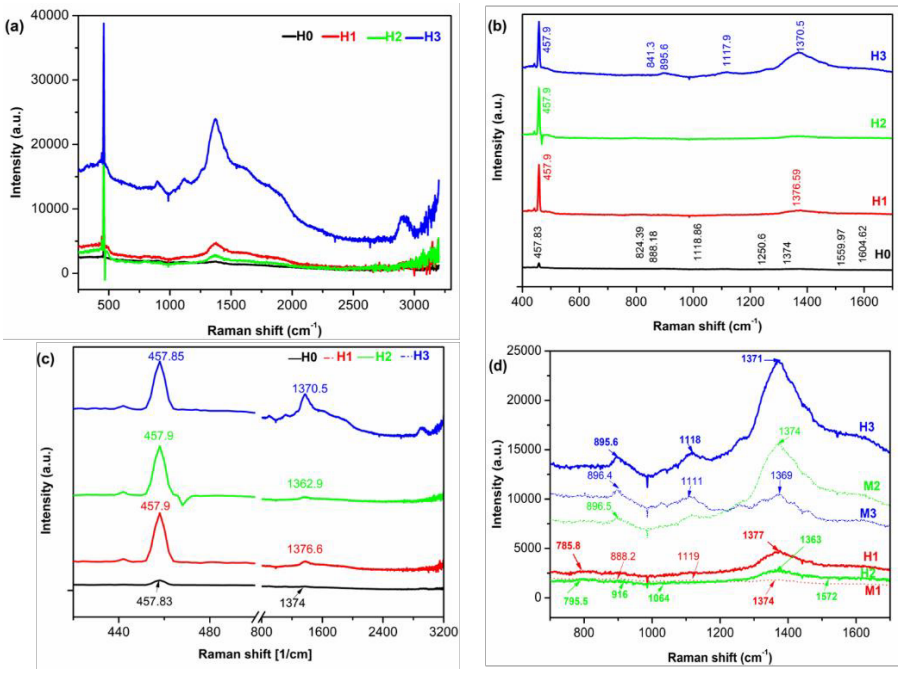

Fig. 7 Raman spectra of the hydrogel matrix H0 (CMC~CA~CSN), and hydrogels H1 (CMC~CA~CSN~β-CD), H2 (2CMC~CA~CSN~β-CD), and H3 (CMC~CA~2CSN~β-CD) showing (a) full spectra, (b) disappeared peaks for H1 and H2 and appeared peaks for H3 in the finger print region, and increased peaks and Raman shifts, (c) in the full spectra and (d) in the finger print region. Increased peak intensities, the appearance of new peaks, and shifts to higher wavenumbers (most notably for H1) indicate fewer defects, interparticle and molecular interaction, structural changes and crosslinking of the hydrogels.

To confirm molecular interaction and crosslinking after inclusion complexation with β-CD, Raman spectroscopy was used to analyze the hydrogels and illustrated in **Fig. 7**. The Raman spectrum of H0 (**Fig. 7**a) show peaks at 342.48 cm^{-1} and 457.83 cm^{-1}, 888.18 cm^{-1}, 1118.9 cm^{-1}, 1374 cm^{-1}, and 2959.8 cm^{-1} which can be assigned strong δ(CC) aliphatic chains, strong υ(O-O) and medium υ(C-O-C), weak υ(C-O-C), δ(CH_3), and strong δ(C-H) vibrations. Within the Raman spectral region characteristic for vibration of aromatic bands (1500-1800 cm^{-1}) and completely free from interfering

bands, β-CD is reported to show peaks at 755 cm^{-1}, 857 cm^{-1}, 925 cm^{-1}, 1050 cm^{-1} and 1085 cm^{-1}, 1132 cm^{-1}, 1331 cm^{-1}, and 1464 cm^{-1}, ascribable to vibrations due to (COO^-), (COO^-) and (CH_3), (CC), (CN), υ(C-O-C), wagging of (CH_2), (CH) and (OH) groups and in-plane bending of (CH_3), (OH), and C=C stretching [56-58]. From **Fig. 7**b and c, it can be seen that the very low intensity bands at 342.5 cm^{-1}, 888.18 cm^{-1}, 1118.9 cm^{-1}, 2552.2 cm^{-1}, 2969.8 cm^{-1} can be observed in the H0 Raman spectrum are absent in the H1 Raman spectrum. This specifies the molecular interaction of H0 with the β-CD surface for hydrogel H1, indicates that the matrix M1 is located within the β-CD cavity and addresses enhanced crosslinking of H1. Also, new peaks (**Fig. 7**b-d) corresponding to 785.83 cm^{-1}, 1377 cm^{-1}, and 3193.8 cm^{-1} relate to β-CD inclusion. As illustrated in **Fig. 7**, shifting, increasing in peak intensities, broadening of characteristic bands, and disappearance of some peaks in the spectra of the developed hydrogels were observed. Sharpness in peak intensities (e.g. at 457.83 cm^{-1} and 1374 cm^{-1}), the disappearance of some peaks and shifts in wavenumbers indicate crystallinity resulting from homogeneity and fewer defects, transformation following chemical interaction/crosslinking, and change in interparticle interaction and chemical bond length of the molecules, respectively. The shorter the bond length, the denser the crosslinks and the greater the shift to higher wavenumber.

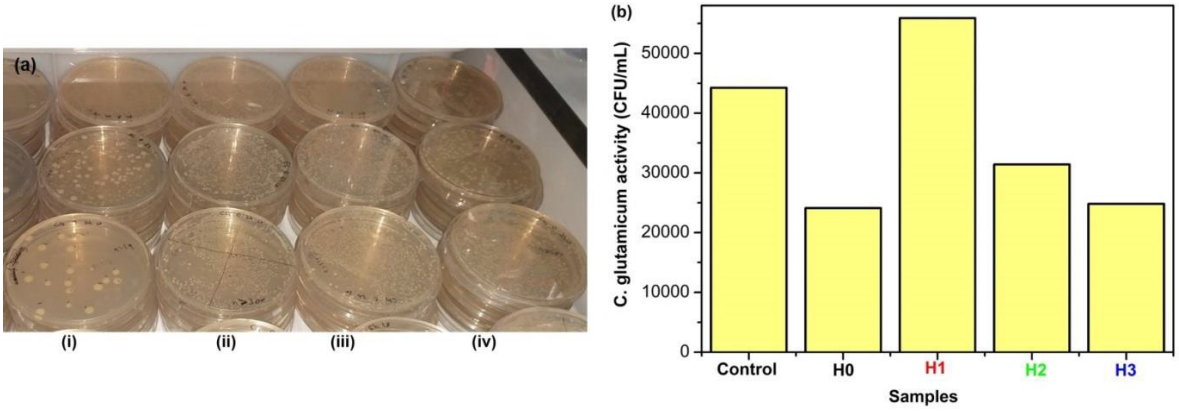

Fig. 8 Viable bacterial counts (CFU/mL). (a) Digital image of the test cultures and their replicates arranged in columns (i) H0, (ii) H1, (iii) H2 and (iv) H3 in LB agar plates. (b) Bacterial counts after 2 h contact time in treated hydrogel matrix H0 (CMC~CA~CSN), and hydrogels H1 (CMC~CA~CSN~β-CD), H2 (2CMC~CA~CSN~β-CD), and H3 (CMC~CA~2CSN~β-CD) compared to untreated sample.

The antimicrobial activity of the optimum hydrogel matrix, H0 and the developed β-CD reinforced hydrogels, H1, H2 and H3 against *C. glutamicum* was studied by dynamic shake flask method and compared with no treatment (without the samples). The results are illustrated in **Fig. 8.** The antimicrobial study shows that while H1 propagated *C. glutamicum* by -26.32%, H2 and H3 show low growth inhibition by 28.99% and 43.95%, respectively when compared with the control sample. And, in 2 h of exposure to *C. glutamicum*, complexation of the hydrogel matrices with β-CD, propagated the bacterium growth by 131.84%, 30.31% and 2.85% for H1, H2, and H3, respectively. This result is similar to those reported that β-CD elicits poor inhibition effect on Gram-positive bacteria activity [41-44]. Thus, this antimicrobial study shows that the optimum hydrogel matrix, H0 is ideal for antimicrobial biomedical application such as wound dressing/treatment while the optimum hydrogel, H1 is suitable for microbial biotechnology application such as metabolic engineering of amino acids.

Following the preceding, the addition of β-CD into CMC-CSN composite matrices crosslinked with CA (1) enhances the degree of crosslinking for H1 and H3, (2) improves gel fraction of all the developed hydrogels , and (3) propagates the growth of Gram-positive bacterium, *C. glutamicum*. Overall, H1 exhibit thermally stable, and well-developed hydrogel microstructure.

4. Conclusion

In this study, non-toxic and environmentally sustainable citric acid (CA) crosslinked carboxymethyl cellulose (CMC) - chitosan (CSN) composite hydrogels matrices were synthesized and characterized for the effect of varying mole ratio of CMC:CSN on hydrolytic properties, crosslinking density, thermal stability, and morphology. Then, to reinforce the matrices, beta-cyclodextrin (β-CD) was incorporated, and the effect of β-CD on the hydrogels' hydrolytic and thermal stability and antibacterial activity was studied. We found that varying mole ratio of CMC and CSN affect hydrogel microstructure. Optimum polymer ratio was at CMC:CSN=1:1, in which hydrolytic stability increased from 63% (CMC~CA~CSN) to 82% (CMC~CA~CSN~β-CD) and thermal stability improved from 4% mass loss (CMC~CA~CSN) to 2.3% mass loss (CMC~CA~CSN~ β-CD) when β-CD was added. Complexation of the hydrogel with β-CD propagated the growth of *C. glutamicum*, the work horse for the production of amino acid and other bio-based chemicals. The study concludes (1) optimal microstructure for a CMC/CSN/CA composite hydrogel is at CMC:CSN = 1:1 in which thermally stable, porous, semi-crystalline hydrogel matrix M1 exhibits optimal hydrolytic properties (495% swelling, 177% water absorbency, and 63% gel fraction); and (2) incorporation of β-CD to CMC-CSN-CA matrix enhances composite hydrogel microstructure and improves hydrogels' hydrolytic stability. Remarkably, this study revealed that well-developed natural bi- polymer-based composite hydrogel microstructure suitable to compete with present- day natural-synthetic polymer-based composite hydrogel could be achieved at a CMC:CSN=1:2. This result is promising for the substitution of petroleum-based polymers with natural polymers for the fabrication of safe, green, composite hydrogels for more widespread applications.

Conflicts of interest

There is no conflict of interest in this work.

Acknowledgements

The study was funded by the Innovation and Technology Commission of Hong Kong (Grant no. PRP/028/19FX) and City University of Hong Kong (Grant no. 9231255, 9667191, 9678189). The authors thank Akintayo Abolude, Quihong Wang, Ejike Onyeukwu, Chuawen Zhou, Chee Kent Lim, Wing Lam Chan and Dr. Patrick Lee for their contributions to the study.

Data availability statement

The raw and processed data required to reproduce these findings cannot be shared at this time as the data forms part of an ongoing study.

References

[1] X. Shen, J.L. Shamshina, P. Berton, G. Gurau, R.D. Rogers, Hydrogels based on cellulose and chitin: fabrication, properties, and applications, Green Chem. 18 (2016) 53-75.

[2] A. Sannino, C. Demitri, M. Madaghiele, Biodegradable Cellulose-based Hydrogels: Design and Applications, Materials 2 (2009) 353-373.

[3] T. Fekete, J. Borsa, E. Takács, L. Wojnárovits, Synthesis of carboxymethylcellulose/starch superabsorbent hydrogels by gamma-irradiation, Chemistry Central Journal 11 (2017).

[4] X. Tong, W. Pan, T. Su, M. Zhang, W. Dong, X. Qi, Recent advances in natural polymer-based drug delivery systems, Reactive and Functional Polymers 148 (2020) 104501.

[5] K. Dharmalingam, R. Anandalakshmi, Fabrication, characterization and drug loading efficiency of citric acid crosslinked NaCMC-HPMC hydrogel films for wound healing drug delivery applications, International Journal of Biological Macromolecules 134 (2019) 815-829.

[6] F. Ullah, M.B. Othman, F. Javed, Z. Ahmad, H. Md Akil, Classification, processing and application of hydrogels: A review, Materials Science and Engineering C Materials for Biological Applications 57 (2015) 414-433.

[7] A. Mignon, N. De Belie, P. Dubruel, S. V. Vlierberghe, Superabsorbent polymers: A review on the characteristics and applications of synthetic, polysaccharide-based, semi-synthetic and 'smart' derivatives, European Polymer Journal 117 (2019) 165 - 178.

[8] C.B. Godiya, S.M. Sayed, Y. Xiao, X. Lu, Highly porous egg white/polyethyleneimine hydrogel for rapid removal of heavy metal ions and catalysis in wastewater, Reactive and Functional Polymers 149 (2020) 104509.

[9] H.W. Kwak, J.E. Kim, K.H. Lee, Green fabrication of antibacterial gelatin fiber for biomedical application, Reactive and Functional Polymers 136 (2019) 86-94.

[10] C. Chang, L. Zhang, Cellulose-based hydrogels: Present status and application prospects, Carbohydrate Polymers 84 (2011) 40-53.

[11] S. Bashir, Y.Y. Teo, S. Ramesh, K. Ramesh, Synthesis and characterization of karaya gum-g- poly (acrylic acid) hydrogels and in vitro release of hydrophobic quercetin, Polymer 147 (2018) 108-120.

[12] J. Shojaeiarani, D. Bajwa, A. Shirzadifar, A review on cellulose nanocrystals as promising biocompounds for the synthesis of nanocomposite hydrogels, Carbohydrate Polymers 216 (2019) 247-259.

[13] X. Zhang, J. Cai, W. Liu, W. Liu, X. Qiu, Synthesis of strong and highly stretchable, electrically conductive hydrogel with multiple stimuli responsive shape memory behavior, Polymer 188 (2020) 122147.

[14] M. Azadi, S. Hassanjili, K. Zarrabi, B. Sarkari, Solidification of hydatid cyst fluid with an injectable chitosan/carboxymethylcellulose/β-glycerophosphate hydrogel for effective control of spillage during aspiration of hydatid cysts, Prog Biomater 7 (2018) 35-54.

[15] L. Song, F. Liu, C. Zhu, A. Li, Facile one-step fabrication of carboxymethyl cellulose based hydrogel for highly efficient removal of Cr(VI) under mild acidic condition, Chemical Engineering Journal 369 (2019) 641-651.

[16] M.I.H. Mondal, Carboxymethyl cellulose. Volume I, Synthesis and characterization, Nova Science Publishers, Incorporated, New York, 2019.

[17] L. Qian, Cellulose-Based Composite Hydrogels: Preparation, Structures, and Applications, in: M.I.H. Mondal (Ed.) Cellulose- Based Hydrogels, Springer International Publishing AG, New York, 2018, pp. 1-50.

[18] S. Khattak, F. Wahid, L.P. Liu, S.R. Jia, L.Q. Chu, Y.Y. Xie, Z.X. Li, C. Zhong, Applications of cellulose and chitin/chitosan derivatives and composites as antibacterial materials: current state and perspectives, Applied Microbiology and Biotechnology 103 (2019) 1989-2006.

[19] M.-C. Li, C. Mei, X. Xu, S. Lee, Q. Wu, Cationic surface modification of cellulose nanocrystals: Toward tailoring dispersion and interface in carboxymethyl cellulose films, Polymer 107 (2016) 200-210.

[20] E. Guibal, T. Vincent, R. Navarro, Metal ion biosorption on chitosan for the synthesis of advanced materials, J Mater Sci 49 (2014) 5505-5518.

[21] M.S. Riaz Rajoka, L. Zhao, H.M. Mehwish, Y. Wu, S. Mahmood, Chitosan and its derivatives: synthesis, biotechnological applications, and future challenges, Applied Microbiology and Biotechnology 103 (2019) 1557-1571.

[22] R. Cheung, T. Ng, J. Wong, W. Chan, Chitosan: An Update on Potential Biomedical and Pharmaceutical Applications, Marine Drugs 13 (2015) 5156-5186.

[23] Y. Bao, J. Ma, N. Li, Synthesis and swelling behaviors of sodium carboxymethyl cellulose-g-poly(AA-co-AM-co-AMPS)/MMT superabsorbent hydrogel, Carbohydrate Polymers 84 (2011) 76-82.

[24] X. Liang, B. Qu, J. Li, H. Xiao, B. He, L. Qian, Preparation of cellulose-based conductive hydrogels with ionic liquid, Reactive and Functional Polymers 86 (2015) 1-6.

[25] R. Jayakumar, D. Menon, K. Manzoor, S.V. Nair, H. Tamura, Biomedical applications of chitin and chitosan based nanomaterials—A short review, Carbohydrate Polymers 82 (2010) 227-232.

[26] E.S. Dragan, M.V. Dinu, Advances in porous chitosan-based composite hydrogels: Synthesis and applications, Reactive and Functional Polymers 146 (2020) 104372.

[27] G. He, W. Ke, X. Chen, Y. Kong, H. Zheng, Y. Yin, W. Cai, Preparation and properties of quaternary ammonium chitosan-g-poly(acrylic acid-co-acrylamide) superabsorbent hydrogels, Reactive and Functional Polymers 111 (2017) 14-21.

[28] C. Deng, X. Lv, Y. Liu, J. Li, W. Lu, G. Du, L. Liu, Metabolic engineering of Corynebacterium glutamicum S9114 based on whole-genome sequencing for efficient N-acetylglucosamine synthesis, Synth Syst Biotechnol 4 (2019) 120-129.

[29] J. Kalinowski, B. Bathe, D. Bartels, N. Bischoff, M. Bott, A. Burkovski, N. Dusch, L. Eggeling, B.J. Eikmanns, L. Gaigalat, A. Goesmann, M. Hartmann, K. Huthmacher, R. Krämer, B. Linke, A.C. McHardy, F. Meyer, B. Möckel, W. Pfefferle, A. Pühler, D.A. Rey, C. Rückert, O. Rupp, H. Sahm, V.F. Wendisch, I. Wiegräbe, A. Tauch, The complete Corynebacterium glutamicum ATCC 13032 genome sequence and its impact on the production of l-aspartate-derived amino acids and vitamins, Journal of Biotechnology 104 (2003) 5-25.

[30] J.Y. Lee, Y.A. Na, E. Kim, H.S. Lee, P. Kim, The Actinobacterium Corynebacterium glutamicum, an Industrial Workhorse, J Microbiol Biotechnol 26 (2016) 807-822.

[31] J. Yang, S. Yang, Comparative analysis of Corynebacterium glutamicum genomes: a new perspective for the industrial production of amino acids, BMC Genomics 18 (2017) 940.

[32] S. Liu, F. Yao, O. Oderinde, K. Li, H. Wang, Z. Zhang, G. Fu, Zinc ions enhanced nacre-like chitosan/graphene oxide composite film with superior mechanical and shape memory properties, Chemical Engineering Journal 321 (2017) 502-509.

[33] L. Upadhyaya, J. Singh, V. Agarwal, R.P. Tewari, Biomedical applications of carboxymethyl chitosans, Carbohydrate Polymers 91 (2013) 452-466.

[34] P. de Cuadro, T. Belt, K.S. Kontturi, M. Reza, E. Kontturi, T. Vuorinen, M. Hughes, Cross-linking of cellulose and poly(ethylene glycol) with citric acid, Reactive and Functional Polymers 90 (2015) 21-24.

[35] V.S. Ghorpade, A.V. Yadav, R.J. Dias, Citric acid crosslinked beta-cyclodextrin/carboxymethylcellulose hydrogel films for controlled delivery of poorly soluble drugs, Carbohydrate Polymers 164 (2017) 339-348.

[36] H. Abou-Yousef, S. Kamel, High efficiency antimicrobial cellulose-based nanocomposite hydrogels, Journal of Applied Polymer Science 132 (2015) 9.

[37] Y.C. Li, M.L. Chen, Synthesis and characterization of curdlan/beta -cyclodextrin composite hydrogels for sustained-release, International Journal of Polymeric Materials and Polymeric Biomaterials 68 (2019) 778-787.

[38] T.R. Hoare, D.S. Kohane, Hydrogels in drug delivery: Progress and challenges, Polymer 49 (2008) 1993-2007.

[39] T.F. Cova, D. Murtinho, A. Pais, A.J.M. Valente, Combining Cellulose and Cyclodextrins: Fascinating Designs for Materials and Pharmaceutics, Front Chem 6 (2018) 271.

[40] N.S. Malik, M. Ahmad, M.U. Minhas, Cross-linked [beta]-cyclodextrin and carboxymethyl cellulose hydrogels for controlled drug delivery of acyclovir, PLoS ONE 12 (2017) e0172727.

[41] H. Van Doorne, E.H. Bosch, C.F. Lerk, Formation and antimicrobial activity of complexes of beta-cyclodextrin and some antimycotic imidazole derivatives, Pharmaceutisch weekblad. Scientific edition 10 (1988) 80-85.

[42] O. Aleem, B. Kuchekar, Y. Pore, S. Late, Effect of beta-cyclodextrin and hydroxypropyl beta-cyclodextrin complexation on physicochemical properties and antimicrobial activity of cefdinir, J Pharm Biomed Anal 47 (2008) 535-540.

[43] M. Calcagnile, S. Bettini, F. Damiano, A. Tala, S.M. Tredici, R. Pagano, M. Di Salvo, L. Siculella, D. Fico, G.E. De Benedetto, L. Valli, P. Alifano, Stimulatory Effects of Methyl-beta-cyclodextrin on Spiramycin Production and Physical-Chemical Characterization of Nonhost@Guest Complexes, ACS Omega 3 (2018) 2470-2478.

[44] C. Dong, L.-Y. Qian, G.-L. Zhao, B.-H. He, H.-N. Xiao, Preparation of antimicrobial cellulose fibers by grafting β-cyclodextrin and inclusion with antibiotics, Materials Letters 124 (2014) 181-183.

[45] E.Y. Yan, X.Y. Hao, M.L. Cao, Y.M. Fan, D.Q. Zhang, W. Xie, J.P. Sun, S.Q. Hou, Preparation and characterization of carboxymethyl chitosan hydrogel, Pigment & Resin Technology 45 (2016) 246-251.

[46] R.A. Lusiana, S. Isdadiyanto, Khabibi, Urea Permeability of Citric Acid Crosslinked Chitosan-Poly (Vinyl Alcohol) Blend Membranes, International Journal of Chemical Engineering and Applications 7 (2016) 186-189.

[47] N.M. Kanafi, N.A. Rahman, N.H. Rosdi, Citric acid cross -linking of highly porous carboxymethyl cellulose/poly(ethylene oxide) composite hydrogel films for controlled release applications, Materials Today: Proceedings 7 (2019) 721-731.

[48] N.S.V. Capanema, A.A.P. Mansur, A.C. de Jesus, S.M. Carvalho, L.C. de Oliveira, H.S. Mansur, Superabsorbent crosslinked carboxymethyl cellulose-PEG

hydrogels for potential wound dressing applications, International Journal of Biological Macromolecules 106 (2018) 17.

[49] M.G. Raucci, M.A. Alvarez-Perez, C. Demitri, D. Giugliano, V. De Benedictis, A. Sannino, L. Ambrosio, Effect of citric acid crosslinking cellulose-based hydrogels on osteogenic differentiation, Journal of Biomedical Materials Research Part A 103 (2015) 2045-2056.

[50] H. Kono, K. Onishi, T. Nakamura, Characterization and bisphenol A adsorption capacity of β-cyclodextrin-carboxymethylcellulose-based hydrogels, Carbohydrate Polymers 98 (2013) 784-792.

[51] S. Bashir, Y.Y. Teo, S. Ramesh, K. Ramesh, Synthesis, characterization, properties of N-succinyl chitosan-g-poly (methacrylic acid) hydrogels and in vitro release of theophylline, Polymer 92 (2016) 36-49.

[52] H.M. Said, S.G. Abd Alla, A.W.M. El-Naggar, Synthesis and characterization of novel gels based on carboxymethyl cellulose/acrylic acid prepared by electron beam irradiation, Reactive and Functional Polymers 61 (2004) 397-404.

[53] K.S.V. Krishna Rao, I. Chung, C.-S. Ha, Synthesis and characterization of poly(acrylamidoglycolic acid) grafted onto chitosan and its polyelectrolyte complexes with hydroxyapatite, Reactive and Functional Polymers 68 (2008) 943-953.

[54] K. Manzoor, M. Ahmad, S. Ahmad, S. Ikram, Removal of Pb(ii) and Cd(ii) from wastewater using arginine cross-linked chitosan–carboxymethyl cellulose beads as green adsorbent, RSC Advances 9 (2019) 7890-7902.

[55] L. Zhang, S. Tang, F. He, Y. Liu, W. Mao, Y. Guan, Highly efficient and selective capture of heavy metals by poly(acrylic acid) grafted chitosan and biochar composite for wastewater treatment, Chemical Engineering Journal 378 (2019) 122215.

[56] M. Ceborska, M. Zimnicka, A.A. Kowalska, K. Dabrowa, B. Repec, Structural diversity in the host-guest complexes of the antifolate pemetrexed with native cyclodextrins: gas phase, solution and solid state studies, Beilstein J Org Chem 13 (2017) 2252-2263.

[57] H. Rachmawati, C.A. Edityaningrum, R. Mauludin, Molecular inclusion complex of curcumin-beta-cyclodextrin nanoparticle to enhance curcumin skin permeability from hydrophilic matrix gel, AAPS PharmSciTech 14 (2013) 1303-1312.

[58] C.S. Mangolim, C. Moriwaki, A.C. Nogueira, F. Sato, M.L. Baesso, A.M. Neto, G. Matioli, Curcumin-beta-cyclodextrin inclusion complex: stability, solubility, characterisation by FT-IR, FT-Raman, X-ray diffraction and photoacoustic spectroscopy, and food application, Food Chem 153 (2014) 361-370.

Supplementary data

Citric acid crosslinked natural bi-polymer-based composite hydrogels: Effect of polymer ratio and beta-cyclodextrin on hydrogel microstructure

Kindness A. Uyanga[a], Oghenefego P. Okpozo[b], Okwuchi S. Onyekwere[c], Walid A. Daoud[a*]

[a] *School of Energy and Environment, City University of Hong Kong, Tat Chee Avenue, Kowloon, Hong Kong*

[b] *School of Engineering, Robert Gordon University, Garthdee, Aberdeen, United Kingdom*

[c] *Faculty of Engineering, Federal University Wukari, Wukari, Taraba State, Nigeria*

This material includes:

Table S1 Comparison of hydrolytic, thermal and structural properties of some CMC or CSN-synthetic hybrid hydrogels with those from this study

Composite hydrogel material	**Solvent/ other synthetic materials**	**Maximum Swelling**	**Gel fraction (insoluble part) in water at 48 h**	**Thermal stability (mass loss at 500 ℃)**	**Nature**	**Ref.**
CSN~CA~PVA membrane	HCl	220%	-	~78%	-	[30]
PVA~CL-1~glutaldehyde	HCl	170 %	-	~87%	Semi-crystalline	[34]
CMC~CA~PEO film	-	2568%	44.17%	~68%	Soft, flexible, amorphous	[31]
Sodium Alginate-chitosan-Arabic gum	Distilled water	207.79%	-	-	-	[35]
CSN~MSN~βGP	Ultrapure water	45.7%	4.5%	-	-	[36]
CMC~CA~CSN	De-ionized water	495%	62.97%	61%	Thin, tough, semi-crystalline	This study
CMC~CA~2CSN	De-ionized water	2200%	84.95%	60.47%	Thin, tough, crystalline	This study

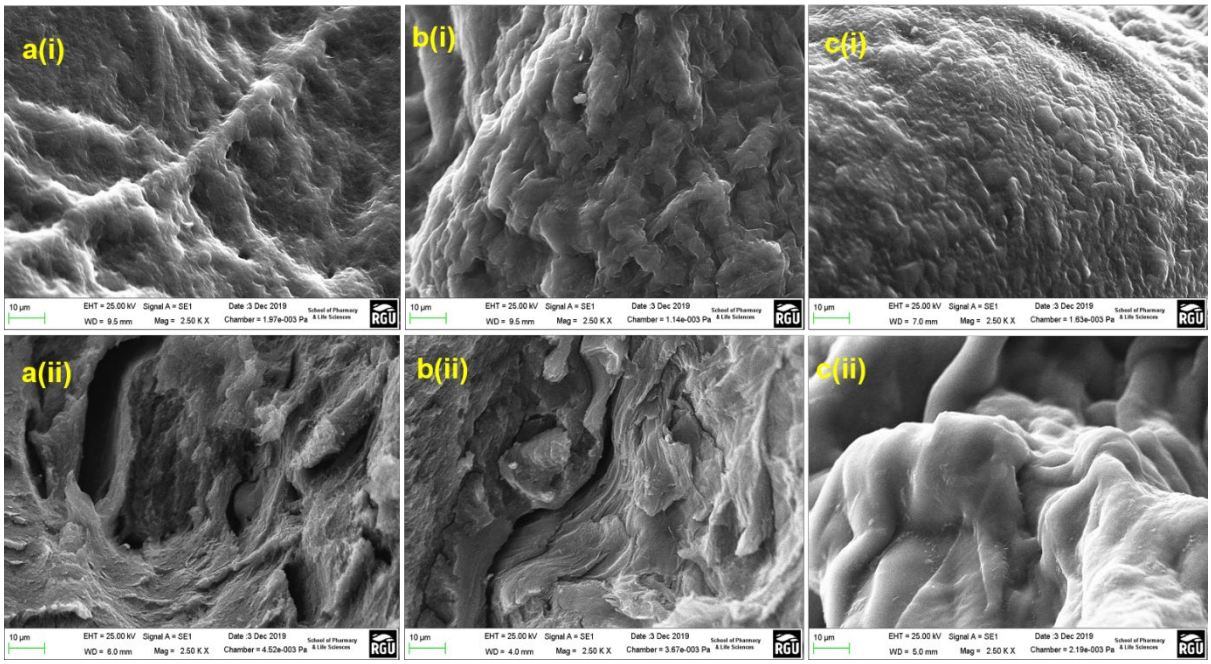

Figure S1 Micrographs of the developed β-CD composite hydrogels (a) CMC~CA~CSN~βCD (H1), (b) 2CMC~CA~CSN~βCD (H2), and (c) CMC~CA~2CSN~βCD (H3) as acquired from (i) top view, and (ii) cross-sectional view